



Older mice show decreased regeneration of neuromuscular junctions following lengthening contraction-induced injury

Thomas A. Paul · Peter C. Macpherson · Tara L. Janetzke · Carol S. Davis · Malcolm J. Jackson · Anne McArdle · Susan V. Brooks 

Received: 11 November 2022 / Accepted: 13 March 2023 / Published online: 23 March 2023
© The Author(s), under exclusive licence to American Aging Association 2023

Abstract Progressive muscle atrophy and loss of muscle strength associated with old age have been well documented. Although age-associated impairments in skeletal muscle regeneration following injury have been demonstrated, less is known about whether aging impacts the regenerative response of neuromuscular junctions (NMJ) following contraction-induced injury. Reduced ability of NMJs to regenerate could lead to increased numbers of denervated muscle fibers and therefore play a contributing role to age-related sarcopenia. To investigate the relationship between age and NMJ regeneration following injury, extensor digitorum longus (EDL) muscles of middle-aged (18–19 months) and old mice (27–28 months) were subjected to a protocol of lengthening contractions (LC) that resulted in an acute force deficit of ~55% as well as functional and histological evidence of a similar magnitude

of injury 3 days post LCs that was not different between age groups. After 28 days, the architecture and innervation of the NMJs were evaluated. The numbers of fragmented endplates increased and of fully innervated NMJs decreased post-injury for the muscle of both middle-aged and old mice and for contralateral uninjured muscles of old compared with uninjured muscles of middle-aged controls. Thus, the diminished ability of the skeletal muscle of old mice to recover following injury may be due in part to an age-related decrease in the ability to regenerate NMJs in injured muscles. The impaired ability to regenerate NMJs may be a triggering factor for degenerative changes at the NMJ contributing to muscle fiber weakness and loss in old age.

T. A. Paul · P. C. Macpherson · T. L. Janetzke · C. S. Davis · S. V. Brooks
Department of Molecular and Integrative Physiology,
University of Michigan, Ann Arbor, MI, USA
e-mail: tompaul@umich.edu

P. C. Macpherson
e-mail: petercdm@med.umich.edu

T. L. Janetzke
e-mail: tjanetz@umich.edu

C. S. Davis
e-mail: csdav@umich.edu

T. A. Paul · S. V. Brooks (✉)
Department of Biomedical Engineering, University
of Michigan, 2029 Biomedical Sciences Building, 109
Zina Pitcher Place, Ann Arbor, MI 48109-2200, USA
e-mail: svbrooks@umich.edu

M. J. Jackson · A. McArdle
MRC-Versus Arthritis Centre for Integrated Research
into Musculoskeletal Ageing (CIMA), Institute of Life
Course and Ageing Science, University of Liverpool,
Liverpool, UK
e-mail: M.J.Jackson@liverpool.ac.uk

A. McArdle
e-mail: mdcr02@liverpool.ac.uk

Keywords Sarcopenia · Neuromuscular junction · Muscle · Aging · Injury · Lengthening contractions · Regeneration · Innervation

Introduction

A high prevalence of sarcopenia, the age-associated loss of muscle mass and strength, is well documented in humans and mice [1] [2]. Losses of muscle mass in humans of ~1% per year from middle age and, in severe cases, a decrease of ~50% of lean muscle mass by the 8th to 9th decade of life have been reported [3]. In addition, the thigh cross-sectional area was shown to be 7.5% smaller for men over the age of 40 years (mean age 52) compared with men under 40 (mean age 31) [4]. While the muscle wasting is clearly a direct contributor to weakness in old age, annual losses in knee extensor strength 3-fold greater than the decreases in thigh lean mass have been documented for both men and women in their 70s [5] indicating that factors other than muscle atrophy are at play in the declining strength.

One mechanism often cited as contributing to both muscle wasting and weakness in old age is the degeneration of neuromuscular junctions (NMJ) and loss of innervation. This conclusion is based largely on numerous observations of an accumulation during aging of NMJs that display morphological abnormalities including partial or complete loss of overlap of pre- and post-synaptic structures and loss of the continuous staining of postsynaptic acetylcholine receptors (AChR), referred to as endplate fragmentation [6]. The factors that trigger the degenerative changes at NMJs are not known, but a diminished ability for NMJs to regenerate in older individuals has been proposed [7, 8]. While muscle injuries are common at all ages, muscles of old animals show increased susceptibility to injury [9–12] and impaired muscle fiber regeneration [13]. Thus, the possibility that impairments with aging in the regeneration of NMJs following muscle injury contribute to the progressive accumulation of degenerating and/or denervated NMJs is a reasonable hypothesis.

Based on the hypothesis that muscles of old animals would demonstrate impairments in NMJ regeneration, Vasilaki et al. [14] proposed that muscles of old mice would show an increase in the number of NMJs displaying abnormal morphology following recovery from muscle injury. This is not what they found. Rather, the pattern of innervation was not different between control and injured

muscles of old mice [14]. Specifically, the proportion of denervated muscle fibers and fragmented NMJs was unchanged by muscle fiber degeneration and regeneration; however, the total number of fibers appearing in muscle cross sections was decreased following the injury. The finding of a loss of fibers from injured muscles of old mice was interpreted as an indicator that muscle regeneration was sufficiently impaired in old age that severely injured fibers experienced a complete failure of regeneration and/or reinnervation and were therefore lost following contraction-induced injury [14]. Thus, the Vasilaki et al. study confirmed impairments in muscle regeneration in old age but left the question of a role of muscle injury as a trigger for NMJ degeneration unresolved.

Muscle weakness by 20–22 months in mice has been reported for some limb muscles, with progressively increasing impairments in force generation along with atrophy occurring thereafter [15, 16]. These observations indicate that factors important for the initiation of sarcopenia are present in mice in middle age. Based on the widely held view that NMJ degeneration and denervation contribute to sarcopenia and the observation that the onset of sarcopenia occurs in middle age, we propose that by inducing injury in middle-aged mice rather than old mice, as in Vasilaki et al. [14], a clearer picture of the role of the impaired NMJ regeneration in the accumulation of NMJs displaying structural abnormalities with increasing age would be revealed. If the age-associated impairments in the ability of NMJs to regenerate are a factor triggering NMJ degeneration, we hypothesized that a bout of severe muscle injury resulting in muscle fiber degeneration and regeneration will increase the number of disrupted NMJs in middle-aged mice. We further hypothesized that the number of degenerating and denervated endplates would increase between the middle (18–19 months) and old (26–28 months) age. To test these hypotheses, we examined NMJ innervation and fragmentation in uninjured control muscles and in muscles 28 days following exposure to a protocol of damaging lengthening contractions in middle-aged and old mice.

Methods

Animals

The animals used for this study were middle-aged (18–19 months) and old (26–28 months) male C57BL/6 mice from our own colony in the University of Michigan Unit for Laboratory Animal

Medicine (ULAM). The mice were housed under specific pathogen-free conditions on a 14:10 light/dark cycle and had ad-libitum access to water and food using the 5LOD chow diet from LabDiet. All animal procedures were approved by the University of Michigan Institutional Animal Care and Use Committee (IACUC).

Lengthening contraction (LC) protocol

To induce a well-defined and reproducible injury, extensor digitorum longus (EDL) muscles were exposed to a protocol of repeated lengthening contractions (LC) during which maximally activated muscles were stretched [17]. Briefly, mice were anesthetized with 3% isoflurane in oxygen. The depth of anesthesia was confirmed by the lack of response to tactile stimuli and was maintained with 2% isoflurane throughout the procedure. Anesthetized mice were placed on a platform maintained at 37 °C, and the hind limb was immobilized by pinning the knee and taping the foot to the platform. Two small incisions were made on the lateral surfaces of the knee and the ankle to expose the peroneal nerve and the distal tendon of the EDL muscle, respectively. The distal tendon was firmly tied to a force transducer (Aurora Scientific Inc. Model 6350) using a 5-0 braided silk suture, and bipolar platinum wire electrodes were placed adjacent and parallel to the nerve. The incision sites were kept moist by warmed sterile saline throughout the duration of the protocol.

The muscle was activated via nerve stimulation with 0.2-ms stimulus pulses, the voltage of which was adjusted to give a maximum isometric twitch. Subsequently, muscle length was adjusted to the optimal length (L_0) for twitch force. With the muscle held at L_0 , 300-ms trains of stimulus pulses were applied at increasing stimulation frequencies until the maximum isometric tetanic force (P_0) was achieved. L_0 was measured with calipers based on well-established anatomical landmarks, and fiber length (L_f) was calculated by multiplying L_0 by the previously determined L_f - L_0 ratio of 0.44 [18]. Muscle physiological cross-sectional area (PCSA) was calculated by dividing muscle mass by the product of L_f and muscle density, 1.06 mg/mm³. Specific P_0 was calculated by dividing P_0 by PCSA. Six mice per age group were exposed to a protocol of LCs

and then allowed to recover for 28 days. A separate group of mice were exposed to LCs and euthanized after 3 days.

The LC protocol consisted of repeated LCs with a contraction every 4 s. Each contraction was 250 ms in duration, and a stretch of 20% strain relative to L_f was initiated 100 ms after the onset of stimulation from near maximum isometric force. Stretches were performed at a strain rate of 1.5 L_f /s. After a 5-min bout of 75 LCs, the muscle was allowed to recover for 5 min, and maximum isometric force was then re-measured. Bouts of LCs were repeated until the maximum isometric force measured following the bout of LCs was reduced to ~50% of the original value of P_0 . The 50% reduction in force required 2 or 3 bouts of LCs and was not different between middle-aged and old mice. After the last bout of LCs, the incisions at the ankle and knee were closed, and mice were observed until ambulatory. Mice were monitored and given buprenorphine for pain every 8–12 h for the first 24 h following injury.

Evaluation of injury

At either 3 or 28 days following the LC protocol, injured/experimental and contralateral control EDL muscles were evaluated for P_0 in vitro with direct muscle fiber activation as previously described [19]. Briefly, mice were anesthetized with an intraperitoneal injection of Avertin, and EDL muscles were isolated, removed, and a 5-0 silk suture was tied to the proximal and distal tendon. Muscles were placed in a horizontal bath containing Krebs Mammalian Ringer solution composed of (in millimolar) 137 NaCl, 5 KCl, 2 CaCl₂·2H₂O, 1 MgSO₄·7H₂O, 1 NaH₂PO₄, 24 NaHCO₃, 11 glucose, and 0.03 tubocurarine chloride. The bath was held at 25 °C and bubbled with 95% O₂ to 5% CO₂ to maintain a pH of 7.4. The proximal tendon was tied to a force transducer (Cambridge Technology model 6650LR), and the distal tendon was tied to a fixed post. Field stimulation (Aurora 701C stimulator) was applied via parallel plate electrodes. Contractile properties were then determined using the same methods described above. Force deficits were calculated in the difference between the P_0 measured for the contralateral control and injured muscles expressed as a percentage of P_0 of the control muscle.

Histological analysis

Upon completion of force measurements, muscles were trimmed of tendons, weighed, and briefly (10 min) fixed in 10% formalin at room temperature. Control and injured muscles were then immersed in tissue freezing medium, frozen in isopentane cooled by liquid nitrogen, and stored at -80°C until sectioning. Flash-frozen EDL muscles were cryo-sectioned at -18°C . Muscles were first positioned to cut transverse sections, and 3 mm of the muscle was sectioned off before obtaining samples for analysis to ensure that the sections contained a maximum number of fibers. Cross sections of a thickness of $10\ \mu\text{m}$ were cut and serially placed on slides. After cross sections were obtained, the remainder of the muscle was repositioned to cut $35\ \mu\text{m}$ thick longitudinal sections, which were also positioned serially on slides. Sectioning was performed serially on five separate slides to avoid double counting the same structure of interest when imaging adjacent sections on a slide. For all animals, the injured and contralateral sections were placed side-by-side on the same slide to ensure there was no inconsistency in the staining protocol between the two conditions. Slides were stored at -20°C until they were stained.

Central nuclei

To confirm that the LC protocol induced widespread muscle fiber injury with degeneration and regeneration, cross sections were analyzed for the presence of centrally located nuclei within myofibers. Sections were rehydrated and blocked for an hour at room temperature using 5% Normal Goat Serum in Phosphate Buffer Saline with 0.2% Triton (PBST). Slides were then incubated overnight with 1:200 anti-rabbit laminin primary antibody (Abcam #7463) to label muscle fiber basal lamina. The following day, slides were washed and incubated with 1:2000 Alexa fluor 555 Goat anti-Rabbit IgG (H+L) secondary antibody (Thermo Fisher #A-21429) for an hour at room temperature. Lastly, slides were incubated with 1:5000 4',6-Diamidino-2-Phenylindole, Dihydrochloride (DAPI, Thermo Fisher D1306) for 5 min at room temperature before being mounted and covered for imaging. Slides from mice euthanized at 3 days post-injury were also stained

with hematoxylin and eosin (H&E) to examine muscle architecture and mononuclear cell infiltration.

Neuromuscular junctions

To visualize the architecture of motor neurons, pre-synaptic terminals, and muscle endplates of injured and contralateral control EDL muscles, longitudinal sections were stained for neurofilament (NF), the abundant synaptic protein, synaptic vesicle protein 2 (SV2), and acetylcholine receptors (AChRs), respectively. To do this, slides were rehydrated and incubated with -20°C 100% methanol for 1 min. Slides were then washed and blocked for an hour at room temperature using 5% Normal Goat Serum and 1:10 ChromPure IgG unconjugated fab fragments (Jackson 015-000-007). Slides were washed and incubated overnight with a primary antibody cocktail consisting of 1:50 SV2A (DSHB SV2) and 1:50 neurofilament (NF-M DSHB 2H3) in PBS with Triton and 5% Normal Goat Serum. The following day, slides were washed and again incubated overnight with 1:2000 Alexa fluor 488 Goat anti-Mouse IgG1 γ 1 secondary antibody (Thermo Fisher AB_2535764) and Alexa fluor 1:2000 594 α -Bungarotoxin (Thermo Fisher B13423). The next day, slides were washed and mounted for imaging.

Imaging and analysis

Fluorescent imaging was performed on a Nikon A1 inverted high-resolution confocal microscope. Images were captured using the NIS Element Viewer software and saved for post-imaging processing and analysis in the FIJI ImageJ software. At $\times 10$ magnification, the borders of individual cross sections were marked, and a stitched image was taken to allow visualization of the entire muscle section. Each image was saved with a randomized file name to prevent observer bias during the analysis. Central nuclei and fiber number were counted from stitched images of muscle cross sections using the MuscleJ [20] macro for NIH ImageJ. The percentage of fibers with central nuclei was calculated by dividing the number of central nuclei per section by the total number of fibers.

Longitudinal sections were analyzed as described in Bhaskaran et. al., [21] with some modifications to provide a clear picture of innervation status and

endplate structure. Z-stack images with a step size of 0.7 μm were taken using a confocal microscope at $\times 20$ magnification. For each animal, at least 50 endplates were analyzed from separate slides and sections to provide a representative sample for the whole EDL muscle. Each image was saved with a randomized file name to prevent bias during the analysis. Using maximum intensity projections for each Z-stack, α -BTX-labeled endplates were identified as either intact or fragmented. A fragmented endplate was defined as one that consisted of at least three islands of AChR clusters that were discontinuous from the other clusters, whereas intact endplates were identified as either displaying a continuous pretzel-shaped pattern of α -BTX staining or limited to two parts of a pattern of AChRs. The total number of fragmented and intact endplates per image was summed and expressed as a percentage of the total number of endplates.

Each NMJ was then categorized as fully innervated, partially innervated, or denervated. A fully innervated NMJ was defined as one where the pre- and post-synaptic staining showed equal to or greater than 95% colocalization, a partially innervated NMJ was characterized by 5–95% colocalization, and a denervated endplate was one that had less than 5% colocalization [21]. The total number of fully innervated, partially innervated, and denervated NMJs per image were summed and expressed as a percentage of the total number of endplates. Upon completion of the fragmentation and innervation analyses, the randomized images were sorted into their respective age group and injury conditions and used to determine an average value for each parameter for each animal. The average values for each animal were used as a single data point for statistical analyses.

Statistical analyses and data presentation

Statistical analyses were conducted using GraphPad Prism 9. Differences between injured and control EDL muscles within a group were tested using two-tailed unpaired *t*-tests. Differences between age groups and injury conditions were tested using a two-way ANOVA with Tukey's post hoc multiple comparisons to establish individual differences. Statistical significance was set a priori at *p* 0.05. Graphical representations were also generated using GraphPad Prism 9.

Results

Initial body masses for the middle-aged (18–19 months) and old (26–28 months) were 36.1 ± 1.7 grams and 33.4 ± 0.7 grams, respectively. After 3 days, body masses were unchanged for both age groups with overall average body masses of $99 \pm 0.1\%$ of the initial values. Similarly, at 28 days, body masses were not different from their respective pre-injury values, at 35.3 ± 1.9 grams for middle-aged and 33.4 ± 0.8 grams for old mice. Maximum isometric forces measured in situ prior to exposure to the lengthening contraction (LC) protocol were 336 ± 20 mN for middle-aged mice and 344 ± 26 mN for the old mice and were not different between the age groups (overall average of 340 ± 16 mN). The decrease in isometric force induced by exposure to LCs is shown in Figure 1A. The decrease is expressed as a force deficit, calculated as the difference between isometric forces generated before and 5 min following the final bout of contractions and expressed as a percentage of the initial maximum isometric force. Consistent with our target, the magnitude of the force deficit was just over our target of 50% (dashed line, Fig. 1A) for both age groups.

The success of the LCs to produce severe injury and muscle fiber degeneration was supported by both functional and morphological evidence obtained from a subset of mice sacrificed 3 days after exposure to the LCs. Three days were chosen based on previous reports that this is the time point when the injury was most severe in this model [22]. The force deficit in the muscles exposed to LCs increased slightly from the value of $\sim 50\%$ observed immediately following the contraction protocol to roughly 55% by 3 days as evidenced by values of specific P_o (sPo) measured in vitro for the injured EDL muscles as compared to the contralateral control muscles (Fig. 1B). No differences were observed between the age groups for the specific forces measured at 3 days for either the muscles exposed to lengthening contractions or the contralateral control muscles, indicating that the magnitude of injury was similar for muscles of middle-aged and old mice. Muscle fiber degeneration was also confirmed by histological examination of the muscles harvested at 3 days. Consistent with the conclusion that the severe force deficits were due to widespread injury and degeneration of the muscles that were not different between middle-aged and old mice,

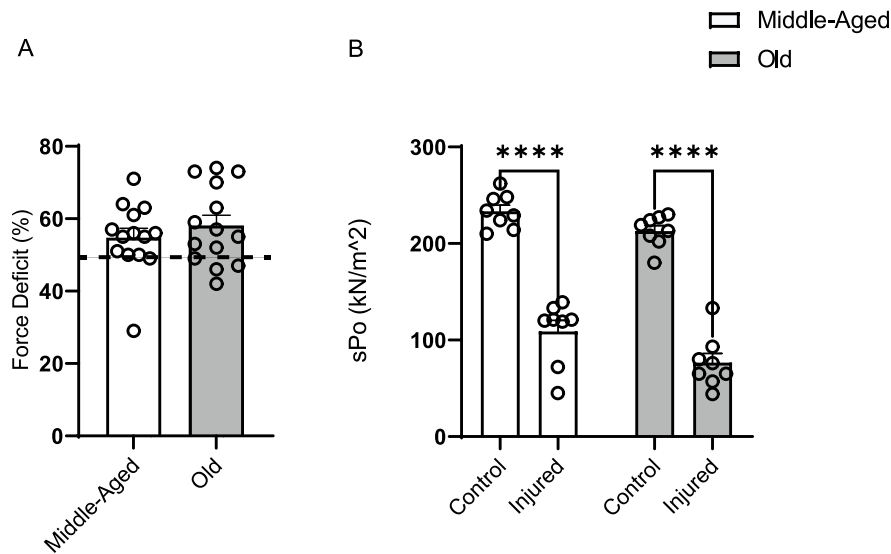


Fig. 1 Force deficits induced by lengthening contractions (LC). **A** shows force deficits for EDL muscles of middle-aged (white bar) and old mice (gray bar) measured *in vivo* immediately following the LC protocol expressed as a percentage of the maximum isometric force measured prior to LCs for each muscle. The dashed line indicates our target force deficit of 50%. **B** shows maximum isometric forces measured *in vitro* for injured and contralateral control EDL muscles from a sub-

set of middle-aged (white bars) and old mice (gray bars) that were sacrificed 3 days after exposure to LCs to verify the presence of injury. No differences were found when comparing injured age groups. Force is normalized by muscle fiber cross-sectional area (specific force). Data were analyzed using a two-way ANOVA with Tukey's multiple comparisons and are presented as individual data points for each muscle along with means \pm SEM. **** indicates $p < 0.0001$

cross sections showed similar levels of necrosis and extensive cellular infiltration in muscles of both age groups exposed to LC (Fig. 2 B, D), which were not observed in contralateral control muscles (Fig. 2 A, C). The number of intact fibers appearing in the cross sections was also quantified from these sections and compared to contralateral uninjured control muscles. For middle-aged and old mice, the numbers of intact fibers in injured muscles were $55 \pm 11\%$ and $58 \pm 10\%$ of numbers in control muscles, respectively. The

similarity in the magnitude of injury allowed us to compare differences in innervation patterns following recovery from injury as an indication of differences between the age groups in NMJ regeneration rather than differences in the severity of the injury-induced.

Twenty-eight days following exposure to LCs, muscle masses and maximum isometric forces were not different between injured and contralateral control muscles for either age group suggesting that the muscles had fully recovered from the damaging

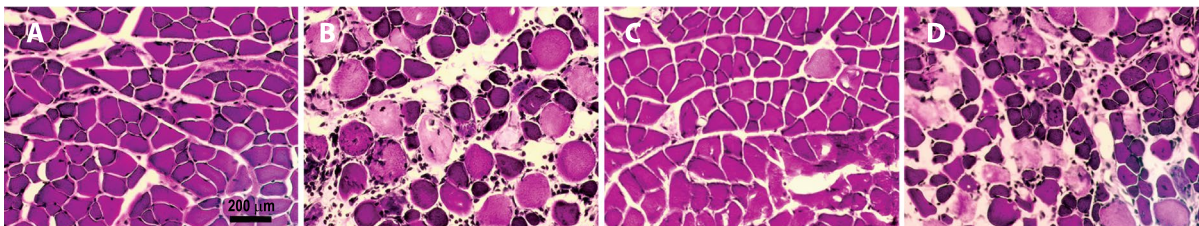


Fig. 2 Histological evidence of injury. **A** and **C** show representative images of cross sections of EDL muscles from uninjured mice, and **B** and **D** show muscles 3 days following exposure to lengthening contractions verifying the presence

of injury and muscle fiber degeneration. Sections in **A** and **B** are from middle-aged mice, and sections in **C** and **D** are from old mice. The scale bar in **A** represents 200 μm and also applies to **B**, **C**, and **D**

contraction protocol at this time point (Fig. 3 A–D). Although in middle-aged mice, absolute P_o recovered to a level that was not significantly different from contralateral control muscles, when values were normalized by muscle cross-sectional areas, specific P_o values were ~20% smaller for injured compared with control muscles (Fig. 3D). The lack of full recovery of specific P_o suggests that not all the mass recovery represented contractile tissue in muscles of middle-aged mice, and muscle fibers were on average weaker than in uninjured control muscles or, alternatively, some fibers were not activated during contractions.

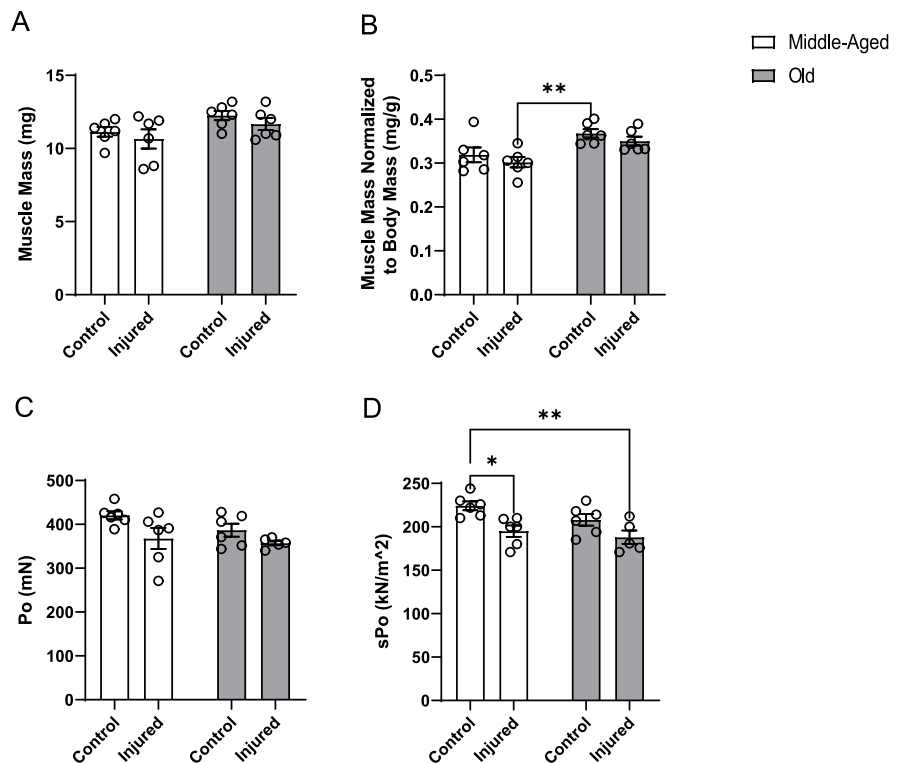
Muscle fiber regeneration was also assessed at 28 days by quantifying the number of fibers in muscle cross sections as well as the number of fibers containing centrally located nuclei (Fig. 4). The total number of muscle fibers present in cross sections was not different between EDL muscles of middle-aged and old mice nor was it impacted by injury for either age group (Fig. 4E). Although total fiber numbers were not different for any of the experimental groups, cross sections of EDL muscles from mice of both age groups showed higher numbers of centrally nucleated fibers in muscles exposed to LCs (Fig. 4

B, D) compared with contralateral control muscles (Fig. 4 A, C). The percentages of centrally nucleated fibers indicate that 25–30% of the fibers in muscles exposed to LC underwent degeneration and regeneration (Fig. 4F).

Longitudinal sections taken from EDL muscles 28 days after exposure to LCs were visualized to examine endplate structure (Fig. 5 A, B). For uninjured control muscles, the extent of endplate fragmentation was nearly 2-fold more severe for muscles of old compared with middle-aged mice. Injured EDL muscles from middle-aged mice also showed higher levels of endplate fragmentation compared with age-matched control muscles, with the fragmentation reaching a level similar to that observed in old control muscles (Fig. 5C). For EDL muscles of old mice, exposure to the LC did not increase the level of endplate fragmentation as old muscles showed no difference in fragmentation between injured and contralateral uninjured control muscles (Fig. 5C).

When examining NMJ innervation status, control muscles of old mice displayed fewer fully innervated NMJs at baseline compared with control muscles of the middle-aged group (Fig. 6D). Muscles

Fig. 3 Functional evaluation of recovery from injury. Data presented for absolute muscle mass in **A**, muscle mass normalized to body mass in **B**, maximum isometric force (P_o) expressed in millinewtons in **C**, and maximum isometric force normalized for muscle fiber cross-sectional area, specific P_o (sP_o) in **D** for control and injured EDL EDL muscles 28 days following lengthening contractions from middle-aged (white bars) and old mice (gray bars). Data were analyzed using a two-way ANOVA with Tukey's multiple comparisons and are presented as individual data points along with means \pm SEM. * indicates $p < 0.05$; ** indicates $p < 0.01$



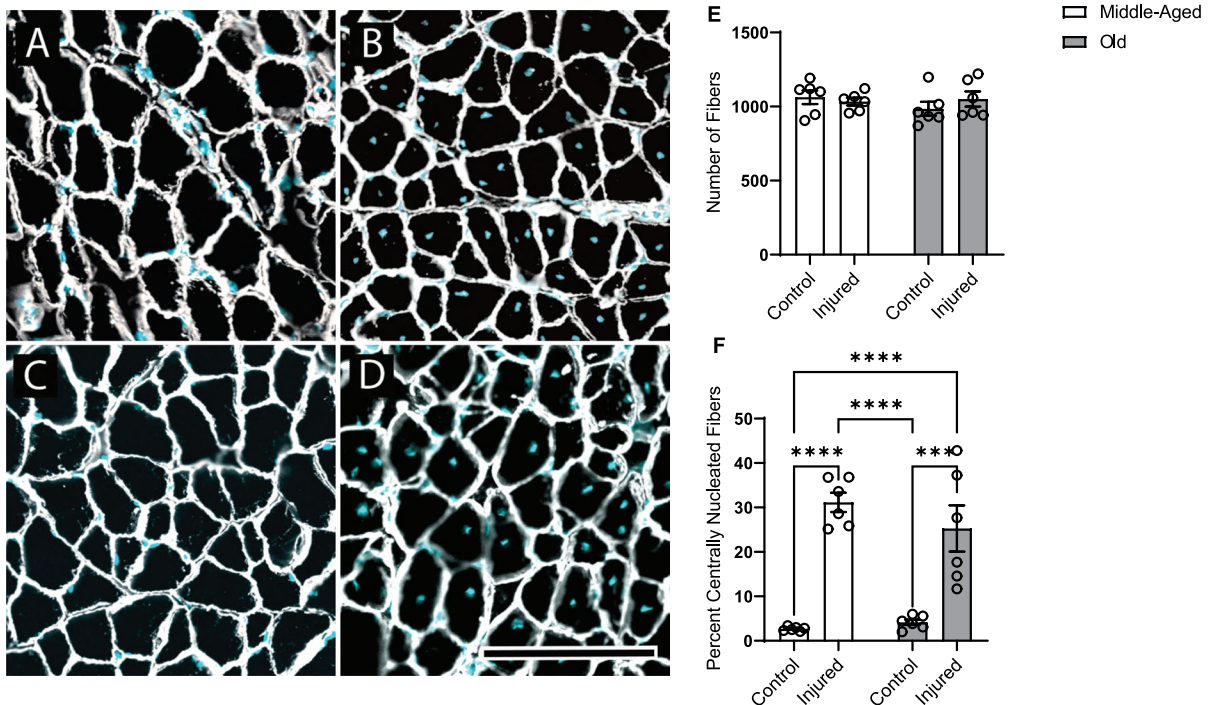


Fig. 4 Histological evidence of regeneration. Representative images are shown for cross sections of EDL muscles 28 days following lengthening contractions (LC). Muscle fiber plasma membrane is visualized using anti-laminin (white) antibody and nuclei are marked with DAPI (cyan). **A** and **C** show contralateral uninjured control muscles of middle-aged and old mice, respectively, and **B** and **D** show injured muscles from middle-aged and old mice, respectively. Central nuclei are apparent inside of the muscle fiber membrane in injured muscles. **E** shows the total number of muscle fibers appearing in cross sec-

tions, and **F** shows the number of fibers with centrally located nuclei expressed as a percentage of the total number of fibers in the sections for uninjured control muscles and injured muscles of middle-aged (white bars) and old mice (gray bars). The scale bar in **D** represents 75 μ m and also applies to **A**, **B**, and **C**. Data were analyzed using a two-way ANOVA with Tukey's multiple comparisons and are presented as individual data points for each muscle along with means \pm SEM. *** indicates $p < 0.001$; **** indicates $p < 0.0001$

of old mice concurrently contained higher levels of partially innervated (Fig. 6E) and denervated endplates (Fig. 6F) than muscles of middle-aged mice. Twenty-eight days following exposure to LCs, EDL muscles of both middle-aged and old mice showed decreases in fully innervated endplates compared with their respective age-matched control muscles (Fig. 6D). In middle-aged animals, this decrease was explained by increases in both partially innervated and fully denervated endplates for injured compared with age-matched control muscles (Fig. 6 E, F), whereas in old mice, the decrease in innervation was coincident with an increase in partially innervated endplates but no significant change in the number of fully denervated NMJs following lengthening contraction-induced injury.

Discussion

With sarcopenia affecting 1 in 10 individuals over the age of 60 [23] and serving as a major contributor to the loss of both mobility and independence in the elderly, an increased understanding of the underlying mechanisms is critical. Denervation-induced loss of muscle fibers is widely accepted as one factor contributing to sarcopenia [6, 24]. Based on the hypothesis that impairments with aging in NMJ regeneration may contribute to muscle fiber denervation, this study examined the structure and innervation status of NMJs in muscles of aging mice following a protocol of lengthening contractions known to cause transient denervation in young mice associated with muscle fiber degeneration and regeneration [14]. Consistent

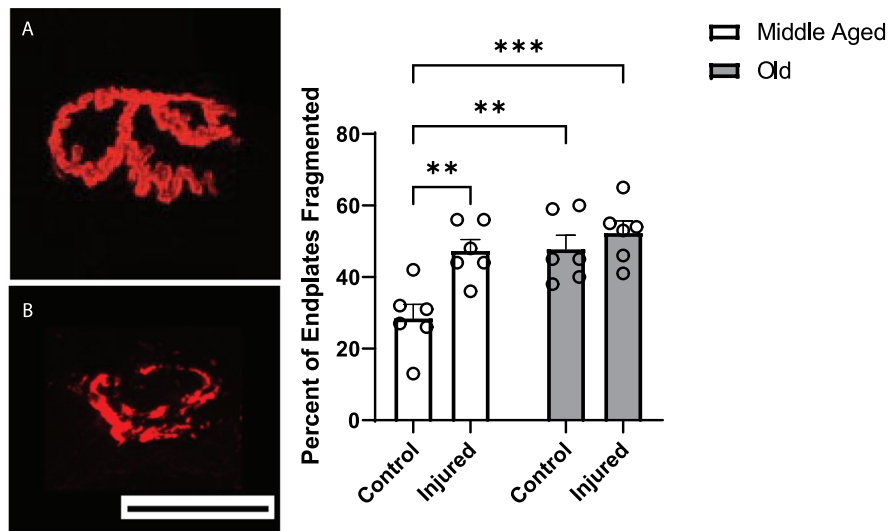


Fig. 5 Analysis of motor endplate fragmentation. **A** shows a representative image of an intact motor endplate that is continuous in structure, and **B** shows a fragmented endplate that contains discontinuous islands of acetylcholine receptors (AChRs). Endplates are visualized with Alexa-594- α -bungarotoxin (red) that labels the AChRs. The scale bar in **B** represents 35 μ m and also applies to **A**. **C** shows the quantification of the number of fragmented endplates expressed as a percentage of the total

number of endplates analyzed for control EDL muscles and injured EDL muscles 28 days following lengthening contractions from middle-aged (white bars) and old mice (gray bars). Data were analyzed using a two-way ANOVA with Tukey's multiple comparisons and are presented as individual data points for each muscle along with means \pm SEM. ** indicates $p < 0.01$; *** indicates $p < 0.001$

with previous literature [21, 25–30] suggesting a role for NMJ degeneration as an early event in age-associated muscle declines, we found significant numbers of NMJs in EDL muscles displaying degenerative changes in middle-aged mice. The middle-aged mice were evaluated at an age (18–19 months) when the EDL muscle does not yet present with atrophy or weakness. Moreover, our observation of higher numbers of fragmented endplates as well as more partially and fully denervated endplates in control muscles of old compared with middle-aged mice is suggestive of progressive NMJ degeneration during aging. We also present the novel result that exposure to muscle injury in middle-aged mice increased the numbers of fragmented endplates as well as partially and fully denervated NMJs to levels seen in control muscles of old mice. These outcomes are significant in light of previous reports suggesting that NMJ disruption may be a causative factor contributing to sarcopenia [6, 31]. The triggers initiating NMJ degeneration are not known, but data from the present study implicate impaired regeneration of NMJs as a possible triggering event that contributes to muscle fiber denervation and loss with aging [8].

Our observation that the muscle fiber and NMJ degeneration and regeneration resulting from lengthening contraction-induced injury did not increase the number of fully denervated or fragmented endplates in 26- to 28-month-old mice is consistent with Vasilaki et al. [14], who reported no change in innervation patterns in muscles of old mice following recovery from contraction-induced damage. Vasilaki et al. [14] also reported that recovery from contraction-induced injury was accompanied by a loss of fibers from cross sections of the muscles in old mice. Their finding is consistent with prior reports of long-term structural and functional deficits, including a loss of fibers, in muscles of old mice following contraction-induced injury [32, 33]. The loss of fibers from injured muscles of old mice has been interpreted as an indicator that muscle regeneration was sufficiently impaired such that some fibers were entirely unable to mount an effective repair response and were completely lost as a result [14]. This interpretation provided the rationale for the present study examining younger middle-aged mice with the hypothesis that impaired recovery of NMJ structure, but not absolute failure of regeneration, would be revealed. Our results support

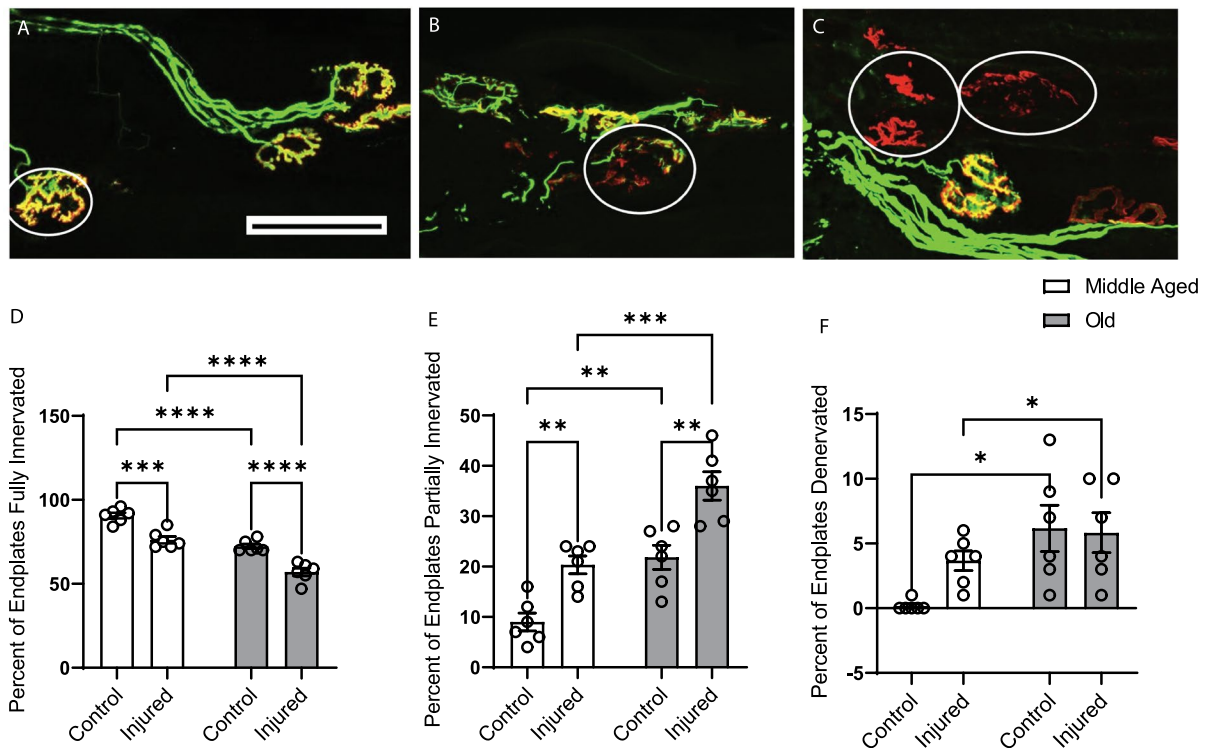


Fig. 6 Analysis of neuromuscular junction (NMJ) innervation. Representative images are shown of NMJs demonstrating our characterization of innervation status. **A** shows a control EDL muscle from a middle-aged animal, and **B** and **C** show control and injured muscles, respectively, from old animals. Nerves are visualized with antibodies for neurofilament and synaptic vesicle protein 2 (green), and acetylcholine receptors are visualized with Alexa-594-α-bungarotoxin (red). White circles indicate fully innervated, partially denervated, and fully denervated

NMJ in **A**, **B**, and **C**, respectively. The scale bar in **A** represents 100 μm and also applies to **B** and **C**. **D**, **E**, and **F** show the quantification of innervation status for control and injured muscles of middle-aged (white bars) and old mice (gray bars). Data were analyzed using a two-way ANOVA with Tukey's multiple comparisons and are presented as individual data points for each muscle along with means ± SEM. * indicates $p < 0.05$; ** indicates $p < 0.01$; *** indicates $p < 0.001$; **** indicates $p < 0.0001$

this notion based on our findings that every aberrant feature of the NMJ morphology analyzed was worsened following muscle fiber degeneration and regeneration in the 18–19 month age group. The muscles also displayed incomplete recovery of muscle-specific force consistent with impaired regeneration and an association between disrupted NMJs and muscle declines, although the present study found no muscle fiber loss due to the injury.

We were somewhat surprised to find that muscles of old mice showed no deficits compared with muscles of middle-aged mice in mass or force. Similar levels of force developed by muscles of mice in both age groups were coincident with greater numbers of disrupted NMJs at the older age, which indicates a disconnect between contractile properties and NMJ

morphology. The essentially “normal” force generation by muscles of old mice with the presence of nearly half of the NMJs displaying some sort of structural deviation from “normal” clearly illustrates that sarcopenic phenotypes cannot be inferred from the presence of NMJs with partial innervation or fragmented endplates. The NMJ is a complex structure with many mechanisms at play in its maintenance. Both pre-synaptic factors, such as the quantal content of neurotransmitter and post-synaptic features including endplate area, AChR density, the extent of postsynaptic folding, and the distribution and density of voltage-dependent sodium channels, all represent potentially modifiable properties to allow consistently reliable neuromuscular transmission [34, 35]. The complex control of NMJ function is highlighted

by the wide variation in the morphology of NMJs across species, between fiber types, and under a wide range of experimental and/or pathological conditions [36]. While the morphological changes to NMJs seen during aging have been interpreted as an indicator of a failure of neuromuscular transmission [6, 37–39], neither direct investigations of age-associated changes in neuromuscular transmission nor in the safety factor of transmission have been reported. To our knowledge, no functional correlates with end-plate fragmentation or partial nerve terminal-AChR overlap have been described to date. This gap adds to the difficulty of interpreting the causal relationship of structural changes to functional consequences. Furthermore, from a theoretical standpoint, there is no reason why a fragmented NMJ should necessarily transmit an action potential any less effective than an NMJ with a pretzel-like morphology [40]. It is possible that a large safety factor allows for full activation during a single maximum isometric contraction, as assessed in the present study, but is not sufficient to support repeated contractions. Although we are only speculating, the fragmentation and partial denervation of NMJs may in fact reduce the safety factor and lead to rundown and impaired neurotransmission during prolonged activity [41, 42]. Such an impairment may contribute to higher susceptibility to fatigue in muscles of old animals [43].

The observation in the present study that the old mice fully recovered muscle mass and maximum isometric force following the lengthening contraction-induced injury is contrary to prior work from our own groups showing prolonged structural and functional deficits in muscles of old mice following contraction-induced injury [14, 32, 33]. Significant variation exists in the literature in the age of onset and rate of progression of sarcopenia. Possible factors that may impact the trajectory of declines in skeletal muscle during aging, including diet formulations, animal breeding and husbandry, and other aspects of the housing conditions across various experimental sites, have been highlighted by criteria established to rigorously test interventions for their impact on lifespan and healthspan [44]. Comparing specific force and mass data in the present study with prior published work [19, 33] supports that the mice examined here resemble adult mice more so than old, but the presence of degenerating and denervated NMJs suggests that the mice are clearly progressing toward

regeneration impairments and may be considered early sarcopenic [25]. In this vein, it is noteworthy that for control uninjured muscles specific force was significantly reduced between middle and old age when the two groups were compared by *t*-test. The presence in both age groups of increased numbers of NMJs displaying morphological abnormalities following lengthening contraction-induced injury raise the possibility that impairments in force production during single or perhaps repeated contractions may have been revealed if muscles had been evaluated *in situ* using nerve stimulation [16].

In addition to our studies using lengthening contractions, NMJ regeneration has been studied following disruptions of innervation induced by nerve crush and by treatment with myotoxins. Consistent with the present findings, recovery of control levels of muscle force and mass in old rodents following injection with myotoxic agents has been reported [45, 46] along with evidence of persistent partial denervation [45]. Following denervation induced by nerve crush, peripheral axons in old mice showed slower regeneration compared with young mice that was associated with a decreased ability to clear the debris left from the degenerating neurons [47]. These studies suggest that there is a diminished ability for aged NMJs to regenerate following damage, but the functional significance of the impairments vary with the severity of the injury and the time following the injury of the evaluation. The potential of targeting the NMJs as a therapeutic strategy for muscle weakness and/or wasting is supported by reports that correcting NMJ defects improves muscle structure and function and attenuates disease progression in pre-clinical models of Duchenne Muscular Dystrophy (DMD) [48]. Although the mechanisms responsible for DMD and sarcopenia are distinct, it is not unreasonable to hypothesize that preserving the integrity of the NMJs would have potential therapeutic benefit to delay or diminish sarcopenia. Moreover, alterations with aging in the dystrophin–glycoprotein complex (DGC) [49] have been reported. These changes appear to contribute to an increased susceptibility to NMJ disruptions following lengthening contractions [50]. The potential role for the DGC in maintaining the integrity of the NMJ raises the possibility that interplay between the DGC and the extracellular matrix (ECM) may also impact NMJ regeneration. Estimates of the volume of ECM from the histological sections stained

for laminin in the present study showed no significant differences between any of our experimental groups; however, we cannot address the question of ECM composition. Thus, an effect of age-associated changes in the quantity of quality of ECM on NMJ degeneration and regeneration cannot be ruled out.

A final question is whether the findings in the present study from the EDL muscle are generalizable to other muscles in particular muscles with different loading histories and potentially different susceptibility to injury. Differences in the habitual loading and usage patterns of a muscle undoubtedly impact susceptibility to injury [51] and potentially NMJ degeneration and regeneration. Although we have not examined any other muscles using the specific interventions and outcomes assessed in the present study, the weight-bearing gastrocnemius muscle shows prolonged structural and functional deficits following lengthening contraction-induced injury [52] as well as accumulation of neuromuscular junctions displaying morphological defects [21], suggesting similar effects of aging on injury and NMJ degeneration may be consistent across different muscles.

In summary, we have shown an increase in the number of NMJs displaying structural abnormalities between middle and old age as well as following exposure of the muscle to an injury that causes muscle fiber degeneration, denervation, and muscle fiber and NMJ regeneration. It has generally been assumed, including in the premise for the present experiment, that the morphological changes to NMJs seen during aging are an indicator of NMJ degeneration that will ultimately lead to full denervation. Alternatively, Slater [40] argues that endplate fragmentation can instead represent the outcome of an active and generally very effective regeneration process. The repair process includes terminal axon sprouting perhaps associated with the differentiation of new postsynaptic regions that help to maintain the efficacy of neuromuscular transmission. The preservation of muscle mass and force in the present study with high levels of fragmented NMJs is consistent with Slater's [40] interpretation that fragmented endplates reflect the ability of these muscles to mount an effective regeneration response. However, as discussed above, the disconnect between contractile properties and NMJ morphology makes extrapolating muscle mass and force based on the extent of NMJ degeneration a tenuous prospect. Further experimentation to clarify

the connection between NMJ morphology and neurotransmission as well as the ultimate impact on muscle function and sarcopenia is clearly warranted.

Author contributions All authors contributed to the study conception and design. Data collection was performed by Thomas Paul, Peter Macpherson, Tara Janetzke, and Carol Davis. Analysis was performed by Thomas Paul and Peter Macpherson. The first draft of the manuscript was written by Thomas Paul, and all authors commented on previous versions of the manuscript. All authors read and approved the final manuscript.

Funding The authors acknowledge the generous funding support from the National Institute on Aging (AG051442) for this work.

Declarations

Conflict of interest The authors declare no competing interests.

Disclaimer The contents do not represent the views of the University of Michigan, the University of Liverpool, the National Institutes of Health, or the US Government.

References

- Rydell-Tormanen K, Johnson JR. The applicability of mouse models to the study of human disease. New York, NY: Humana Press; 2019. https://doi.org/10.1007/978-1-4939-9086-3_1.
- Xie WQ, He M, Yu DJ, Wu YX, Wang XH, Lv S, Xiao WF, Li YS. Mouse models of sarcopenia: classification and evaluation. *J Cachexia Sarcopenia Muscle*. 2021;12:538–54. <https://doi.org/10.1002/jcsm.12709>.
- Wilkinson DJ, Piasecki M, Atherton PJ. The age-related loss of skeletal muscle mass and function: Measurement and physiology of muscle fibre atrophy and muscle fibre loss in humans. *Ageing Res Rev*. 2018;47:123–32. <https://doi.org/10.1016/j.arr.2018.07.005>.
- Keller K, Engelhardt M. Strength and muscle mass loss with aging process. Age and strength loss. *Muscles Ligaments Tendons J*. 2013;3:346–50.
- Goodpaster BH, Park SW, Harris TB, Kritchevsky SB, Nevitt M, Schwartz AV, Simonsick EM, Tylavsky FA, Visser M, Newman AB. The loss of skeletal muscle strength, mass, and quality in older adults: the health, aging and body composition study. *J Gerontol A Biol Sci Med Sci*. 2006;61:1059–64. <https://doi.org/10.1093/gerona/61.10.1059>.
- Jang YC, Van Remmen H. Age-associated alterations of the neuromuscular junction. *Exp Gerontol*. 2011;46:193–8. <https://doi.org/10.1016/j.exger.2010.08.029>.
- Doherty TJ, Vandervoort AA, Brown WF. Effects of ageing on the motor unit: a brief review. *Can J Appl Physiol*. 1993;18:331–58. <https://doi.org/10.1139/h93-029>.
- Sonjak V, Jacob K, Morais JA, Rivera-Zengotita M, Spendiff S, Spake C, Taivassalo T, Chevalier S, Hoppel RT. Fidelity of muscle fibre reinnervation modulates ageing muscle impact in elderly women. *J Physiol*. 2019;597:5009–23. <https://doi.org/10.1113/JP278261>.

9. Choi SJ, Lim JY, Nibaldi EG, Phillips EM, Frontera WR, Fielding RA, Widrick JJ. Eccentric contraction-induced injury to type I, IIa, and IIa/IIx muscle fibers of elderly adults. *Age (Dordr)*. 2012;34:215–26. <https://doi.org/10.1007/s11357-011-9228-2>.
10. Hettinger ZR, Hamagata K, Confides AL, Lawrence MM, Miller BF, Butterfield TA, Dupont-Versteegden EE. Age-related susceptibility to muscle damage following mechanical therapy in rats recovering from disuse atrophy. *J Gerontol A Biol Sci Med Sci*. 2021;76:2132–40. <https://doi.org/10.1093/gerona/glab186>.
11. Manfredi TG, Fielding RA, O'Reilly KP, Meredith CN, Lee HY, Evans WJ. Plasma creatine kinase activity and exercise-induced muscle damage in older men. *Med Sci Sports Exerc*. 1991;23:1028–34.
12. Ploutz-Snyder LL, Giamis EL, Formikell M, Rosenbaum AE. Resistance training reduces susceptibility to eccentric exercise-induced muscle dysfunction in older women. *J Gerontol A Biol Sci Med Sci*. 2001;56:B384–B90. <https://doi.org/10.1093/gerona/56.9.b384>.
13. Volpi E, Nazemi R, Fujita S. Muscle tissue changes with aging. *Curr Opin Clin Nutr Metab Care*. 2004;7:405–10. <https://doi.org/10.1097/01.mco.0000134362.76653.b2>.
14. Vasilaki A, Pollock N, Giakoumaki I, Goljanek-Whysall K, Sakellariou GK, Pearson T, Kayani A, Jackson MJ, McArdle A. The effect of lengthening contractions on neuromuscular junction structure in adult and old mice. *Age (Dordr)*. 2016;38:259–72. <https://doi.org/10.1007/s11357-016-9937-7>.
15. Kim C, Hwang JK. The 5,7-dimethoxyflavone suppresses sarcopenia by regulating protein turnover and mitochondria biogenesis-related pathways. *Nutrients*. 2020;12:1079. <https://doi.org/10.3390/nu12041079>.
16. Larkin LM, Davis CS, Sims-Robinson C, Kostrominova TY, Van Remmen H, Richardson A, Feldman EL, Brooks SV. Skeletal muscle weakness due to deficiency of CuZn-superoxide dismutase is associated with loss of functional innervation. *Am J Physiol Regul Integr Comp Physiol*. 2011;301:R1400–7. <https://doi.org/10.1152/ajpregu.00093.2011>.
17. Koh TJ, Peterson JM, Pizza FX, Brooks SV. Passive stretches protect skeletal muscle of adult and old mice from lengthening contraction-induced injury. *J Gerontol A Biol Sci Med Sci*. 2003;58:592–7. <https://doi.org/10.1093/gerona/58.7.B592>.
18. Brooks SV. Rapid recovery following contraction-induced injury to *in situ* skeletal muscles in *mdx* mice. *J Muscle Res Cell Mot*. 1998;19:179–87. <https://doi.org/10.1023/a:1005364713451>.
19. Brooks SV, Faulkner JA. Contractile properties of skeletal muscles from young, adult and aged mice. *J Physiol*. 1988;404:71–82. <https://doi.org/10.1113/jphysiol.1988.sp017279>.
20. Mayeuf-Louchart A, Hardy D, Thorel Q, Roux P, Gueniot L, Briand D, Mazeraud A, Bougle A, Shorte SL, Staels B, Chretien F, Duez H, Danckaert A. Muscledj: a high-content analysis method to study skeletal muscle with a new Fiji tool. *Skelet Muscle*. 2018;8:25. <https://doi.org/10.1186/s13395-018-0171-0>.
21. Bhaskaran S, Pollock N, Macpherson PCD, Ahn B, Piekarz KM, Staunton CA, Brown JL, Qaisar R, Vasilaki A, Richardson A, McArdle A, Jackson MJ, Brooks SV, Van Remmen H. Neuron-specific deletion of CuZn-SOD leads to an advanced sarcopenic phenotype in older mice. *Aging Cell*. 2020;19:e13225. <https://doi.org/10.1111/acer.13225>.
22. McCully KK, Faulkner JA. Injury to skeletal muscle fibers of mice following lengthening contractions. *J Appl Physiol*. 1985;59:119–26. <https://doi.org/10.1152/jappl.1985.59.1.119>.
23. Shafiee G, Keshtkar A, Soltani A, Ahadi Z, Larijani B, Heshmat R. Prevalence of sarcopenia in the world: a systematic review and meta-analysis of general population studies. *J Diabetes Metab Disord*. 2017;16:21. <https://doi.org/10.1186/s40200-017-0302-x>.
24. Gonzalez-Freire M, de Cabo R, Studenski SA, Ferrucci L. The neuromuscular junction: aging at the crossroad between nerves and muscle. *Front Aging Neurosci*. 2014;6:208. <https://doi.org/10.3389/fnagi.2014.00208>.
25. Balice-Gordon RJ. Age-related changes in neuromuscular innervation. *Muscle Nerve Suppl*. 1997;5:S83–7. [https://doi.org/10.1002/\(SICI\)1097-4598\(1997\)5+%3C83::AID-MUS20%3E3.0.CO;2-Z](https://doi.org/10.1002/(SICI)1097-4598(1997)5+%3C83::AID-MUS20%3E3.0.CO;2-Z).
26. Cardasis CA, LaFontaine DM. Aging rat neuromuscular junctions: a morphometric study of cholinesterase-stained whole mounts and ultrastructure. *Muscle & Nerve*. 1987;10:200–13. <https://doi.org/10.1002/mus.880100303>.
27. Fahim MA, Holley JA, Robbins N. Scanning and light microscopic study of age changes at a neuromuscular junction in the mouse. *J Neurocytol*. 1983;12:13–25. <https://doi.org/10.1007/bf01148085>.
28. Fahim MA, Robbins N. Ultrastructural studies of young and old mouse neuromuscular junctions. *J Neurocytol*. 1982;11:641–56. <https://doi.org/10.1007/bf01262429>.
29. Oda K. Age changes of motor innervation and acetylcholine receptor distribution on human skeletal muscle fibres. *J Neurol Sci*. 1984;66:327–38. [https://doi.org/10.1016/0022-510X\(84\)90021-2](https://doi.org/10.1016/0022-510X(84)90021-2).
30. Wokke JH, Jennekens FG, van den Oord CJ, Veldman H, Smit LM, Leppink GJ. Morphological changes in the human end plate with age. *J Neurol Sci*. 1990;95:291–310. [https://doi.org/10.1016/0022-510X\(90\)90076-Y](https://doi.org/10.1016/0022-510X(90)90076-Y).
31. Chai RJ, Vukovic J, Dunlop S, Grounds MD, Shavlakadze T. Striking denervation of neuromuscular junctions without lumbar motoneuron loss in geriatric mouse muscle. *PLoS One*. 2011;6:e28090. <https://doi.org/10.1371/journal.pone.0028090>.
32. Brooks SV, Faulkner JA. Contraction-induced injury: recovery of skeletal muscles in young and old mice. *Am J Physiol*. 1990;258:C436–42. <https://doi.org/10.1152/ajpce.11.1990.258.3.C436>.
33. McArdle A, Dillmann WH, Mestrlil R, Faulkner JA, Jackson MJ. Overexpression of HSP70 in mouse skeletal muscle protects against muscle damage and age-related muscle dysfunction. *FASEB J*. 2004;18:355–7. <https://doi.org/10.1096/fj.03-0395fj>.
34. Girard E, Barbier J, Chatonnet A, Krejci E, Molgo J. Synaptic remodeling at the skeletal neuromuscular junction of acetylcholinesterase knockout mice and its physiological relevance. *Chem Biol Interact*. 2005;157:158:87–96. <https://doi.org/10.1016/j.cbi.2005.10.010>.
35. Rogozhin AA, Pang KK, Bukharaeva E, Young C, Slater CR. Recovery of mouse neuromuscular junctions from single and repeated injections of botulinum neurotoxin A. *J Physiol*. 2008;586:3163–82. <https://doi.org/10.1113/jphysiol.2008.153569>.

36. Wood SJ, Slater CR. Safety factor at the neuromuscular junction. *Prog Neurobiol*. 2001;64:393–429. [https://doi.org/10.1016/S0301-0082\(00\)00055-1](https://doi.org/10.1016/S0301-0082(00)00055-1).
37. Deschenes MR, Roby MA, Glass EK. Aging influences adaptations of the neuromuscular junction to endurance training. *Neuroscience*. 2011;190:56–66. <https://doi.org/10.1016/j.neuroscience.2011.05.070>.
38. Rudolf R, Khan MM, Labeit S, Deschenes MR. Degeneration of neuromuscular junction in age and dystrophy. *Front Aging Neurosci*. 2014;6:99. <https://doi.org/10.3389/fnagi.2014.00099>.
39. Valdez G, Tapia JC, Lichtman JW, Fox MA, Sanes JR. Shared resistance to aging and ALS in neuromuscular junctions of specific muscles. *PLoS One*. 2012;7:e34640. <https://doi.org/10.1371/journal.pone.0034640>.
40. Slater CR. 'Fragmentation' of NMJs: a sign of degeneration or regeneration? A long journey with many junctions. *Neuroscience*. 2020;439:28–40. <https://doi.org/10.1016/j.neuroscience.2019.05.017>.
41. Shi Y, Ivannikov MV, Walsh ME, Liu Y, Zhang Y, Jaramillo CA, Macleod GT, Van Remmen H. The lack of CuZnSOD leads to impaired neurotransmitter release, neuromuscular junction destabilization and reduced muscle strength in mice. *PLoS One*. 2014;9:e100834. <https://doi.org/10.1371/journal.pone.0100834>.
42. Zhao K, Shen C, Li L, Wu H, Xing G, Dong Z, Jing H, Chen W, Zhang H, Tan Z, Pan J, Xiong L, Wang H, Cui W, Sun XD, Li S, Huang X, Xiong WC, Mei L. Sarcoglycan alpha mitigates neuromuscular junction decline in aged mice by stabilizing LRP4. *J Neurosci*. 2018;38:8860–73. <https://doi.org/10.1523/JNEUROSCI.0860-18.2018>.
43. Fogarty MJ, Gonzalez Porras MA, Mantilla CB, Sieck GC. Diaphragm neuromuscular transmission failure in aged rats. *J Neurophysiol*. 2019;122:93–104. <https://doi.org/10.1152/jn.00061.2019>.
44. Strong R, Miller RA, Cheng CJ, Nelson JF, Gelfond J, Allani SK, Diaz V, Dorigatti AO, Dorigatti J, Fernandez E, Galecki A, Ginsburg B, Hamilton KL, Javors MA, Kornfeld K, Kaerberlein M, Kumar S, Lombard DB, Lopez-Cruzan M, et al. Lifespan benefits for the combination of rapamycin plus acarbose and for captopril in genetically heterogeneous mice. *Aging Cell*. 2022;21:e13724. <https://doi.org/10.1111/accel.13724>.
45. Carlson BM, Dedkov EI, Borisov AB, Faulkner JA. Skeletal muscle regeneration in very old rats. *J Gerontol*. 2001;56A:B1–B10. <https://doi.org/10.1093/gerona/56.5.B224>.
46. Lee AS, Anderson JE, Joya JE, Head SI, Pather N, Kee AJ, Gunning PW, Hardeman EC. Aged skeletal muscle retains the ability to fully regenerate functional architecture. *Bioarchitecture*. 2013;3:25–37. <https://doi.org/10.4161/bioa.24966>.
47. Kang H, Lichtman JW. Motor axon regeneration and muscle reinnervation in young adult and aged animals. *J Neurosci*. 2013;33:19480–91. <https://doi.org/10.1523/JNEUROSCI.4067-13.2013>.
48. Ng SY, Ljubcic V. Recent insights into neuromuscular junction biology in Duchenne muscular dystrophy: impacts, challenges, and opportunities. *EBioMedicine*. 2020;61:103032. <https://doi.org/10.1016/j.ebiom.2020.103032>.
49. Rice KM, Preston DL, Neff D, Norton M, Blough ER. Age-related dystrophin-glycoprotein complex structure and function in the rat extensor digitorum longus and soleus muscle. *J Gerontol A Biol Sci Med Sci*. 2006;61:1119–29. <https://doi.org/10.1093/gerona/61.11.1119>.
50. Hughes DC, Marcotte GR, Marshall AG, West DWD, Baehr LM, Wallace MA, Saleh PM, Bodine SC, Baar K. Age-related differences in dystrophin: impact on force transfer proteins, membrane integrity, and neuromuscular junction stability. *J Gerontol A Biol Sci Med Sci*. 2017;72:640–8. <https://doi.org/10.1093/gerona/glw109>.
51. Faulkner JA, Jones DA, Round JM. Injury to skeletal muscles of mice by forced lengthening during contractions. *Q J Exp Physiol*. 1989;74:661–70. <https://doi.org/10.1113/expphysiol.1989.sp003318>.
52. Rader EP, Faulkner JA. Recovery from contraction-induced injury is impaired in weight-bearing muscles of old male mice. *J Appl Physiol*. 2006;100:656–61. <https://doi.org/10.1152/jappphysiol.00663.2005>.

Publisher's note Springer Nature remains neutral with regard to jurisdictional claims in published maps and institutional affiliations.

Springer Nature or its licensor (e.g. a society or other partner) holds exclusive rights to this article under a publishing agreement with the author(s) or other rightsholder(s); author self-archiving of the accepted manuscript version of this article is solely governed by the terms of such publishing agreement and applicable law.